A Flexible Robotics-inspired Computational Model of Compressive Loading on the Human Spine

Leonardo Ventura[1], Marta Lorenzini[1], Wansoo Kim[1,2], Arash Ajoudani[1]

***Abstract*— The use of powerful robotics tools in modeling and analysis of complex biomechanical systems has led to the development of computationally effective and scalable human models. Our early work in this regard focused on a humanoids-based rigid-body modeling of human kinodynamics to monitor instantaneous and accumulating effects of external loads on body joints. Nevertheless, despite their high-computational efficiency, the flexible nature of the spine and its characteristic were not taken into account, resulting in less accurate estimations of the spinal compressive forces. Accordingly, in this work, we propose a flexible model of the human spine mechanics for assessing compressive loading, and integrate it in our robotics-based whole-body model. Such a model can quantify the compressive force distribution along the spine and the muscles' activity for a measured back configuration and known external forces, which both contribute to increasing the ergonomic risk level. The muscles' activity predictions are validated through an experimental analysis on six human subjects. Three different tests are conducted considering different loading conditions. Results demonstrate the potential of the proposed approach in monitoring the spine compressive loading and predicting a muscles activity with an average accuracy of 10% against experimental data. Minimizing the required number of sensors and the amount of computational resources, the presented approach is particularly suitable for online risk evaluation in a real working scenario.**

Keywords: Modeling and Simulating Humans; Human Factors and Human-in-the-Loop; Human-Centered Robotics.

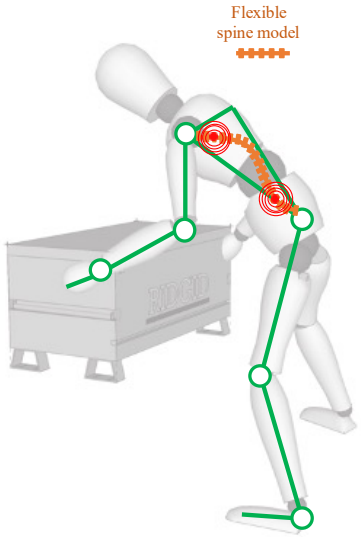

Fig. 1: The simplified model to represent the human body enriched with a flexible model of the spine to take into account the compressive force distribution due to external loads.

I. INTRODUCTION

Musculoskeletal disorders (MSDs) are one of the most frequent causes of work-related illness. The International Labour Organization estimates that MSDs affect tens of millions of workers across all employment sectors [1]. Giving rise to physical issues (i.e. chronic pain and functional impairment) and physiological diseases [2], MSDs are among the major problems in both developed and developing countries. In the European Union, their economic impact represents the 2% of gross domestic product [3]. In particular, Low back pain (LBP) is the second most common pain condition [4] and is the most frequent MSDs [5].

A high-potential solution to the prevention and mitigation of MSDs in the workplace is represented by collaborative robots (cobots). From a physical point of view, cobots can facilitate a reduction of biomechanical overload by supporting operators in heavy and repetitive tasks [6]. In addition, they can lead to more flexible production systems while minimizing fixed costs and layout changes thus they are increasingly employed in manufacturing systems [7]. Nevertheless, humans supervision and decisions making capability remain crucial and physical interactions between cobots and operators are often required, as in co-manipulation [8], [9] or co-carrying [10], [11] tasks.

To promote human-centred collaborative frameworks, online methods for assessing the effect of external loading on all body joints [12], [13] and fatigue [14], [15] in human-robot collaborations have been developed and their effectiveness have been evaluated [16], [17] in our previous works. By employing the principles of humanoid robotics to model human kinematics, dynamics and effort, the proposed methods allow reduced complexity but increased scalability, showing promising opportunities for workers' physical load assessment. Indeed, they feature a significantly low computational cost and fast-identifiable human model, meeting the requirements of real industrial factories. However, fully rigid systems can well-approximate human tasks kinematics, but they largely simplify the human body mechanics and are not suitable to estimate the internal forces distribution and its effects on specific body districts. Therefore, integrating flexible links can lead to more appropriate results, fosters subject-specific approaches and advancing our research in

[1]Leonardo Ventura, Marta Lorenzini, Wansoo Kim and Arash Ajoudani are with Human-Robot Interfaces and Physical Interaction Lab (HRI[2]), Istituto Italiano di Tecnologia, Genoa, Italy leonardo.ventura@iit.it

[2]Wansoo Kim is with Hanyang University, Republic of Korea

the assessment of workers' ergonomics (see Figure 1).

The flexible nature of the human spine and its characteristic stress-free configuration play a crucial role in sustaining a certain body configuration. During lifting and carrying tasks, the lower back is under exceptional compressive loading and compressive forces are the primary cause of the pain due to fracture of the vertebral endplate [18]. Accordingly, this paper aims to introduce a model for assessing online compressive loading acting along the human spine.

Although direct measures are possible to address spine compressive loading [19], they are not applicable for preventive purposes. Thus, the two common strategies available in the literature are deductive Finite Element Method (FEM) models [20], [21], [22] and inductive electromyography (EMG) driven models [23], [24], [25]. Both approaches can result in a compressive loading similar to in vivo measurements [26]. Nevertheless, none of them is applicable in real working scenarios. FEM models require large computational power and are not suitable for online estimation. Moreover, the model definition requires a large amount of data difficult to access [27]. This makes them unsuitable when aiming at a large number of subjects. On the other hand, EMG-driven approaches are available at a small computational cost and are easier to be customized for several subjects. Nevertheless, the required EMG sensors limit their feasibility due to workers discomfort, excessive set-up time and sensitivity to sweat, hair, and sensor placement.

Recently, a Spine Equivalent Beam (SEB) model has been proposed [28]. It requires a very limited set of inputs (subject's height and weight) but can be further specialized on-demand. The model solution can be numerically obtained with low computational complexity, and the predicted compressive forces are validated against in-vivo measurements during a full flexion cycle. However, external loads in lifting and carrying tasks are not taken into account in the model definition. We focus on real-world scenarios where handling heavy objects may be linked to MSDs risk factors. Intuitively, any handled object has a direct effect on the spine. It results in an additional loading balanced by a greater ground reaction force. Placed between these two applications points, the spine experiences larger compressive stresses that depend on both external action and human body configuration. Furthermore, as the external load increases the antagonistic muscles contraction stiffens the trunk [29] increasing spine stability [30]. Both the direct effect of external loads and the increased muscle activity contributes to spine loading and must be considered for ergonomic risk assessment.

This work provides a practical tool for preventing back-related MSDs. We present an extended SEB model including the effect of external loads and the estimated Erector-Spine (ES) muscles activity. The muscles effort required to retain a certain configuration under an external load is computed numerically and validated against experimental data. Therefore, the risk associated with a specific spine configuration and a known external load can be feedback while conducting physically demanding tasks without the need for cumbersome acquisition systems or large computational cost, hence it will be suitable for use in the online assessment method.

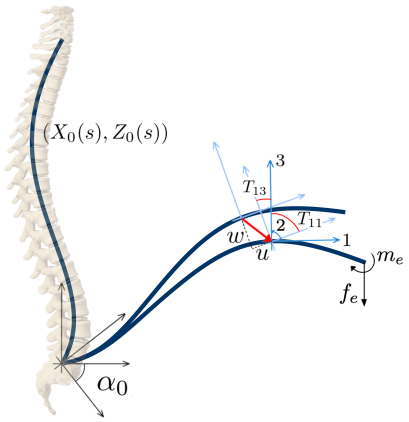

Fig. 2: The stress-free configuration of the spine described as a 2D curve, $(X_0(s), Z_0(s))$, rotate in the sagittal plane of an angle α_0. Knowing α_0, the deformed coordinate system, $_{123}$, is uniquely defined by two displacements (u, w) and one of the two rotations (T_{11}, T_{13}).

The paper is organized as follows. First, the simplified model of the spine is described in the next section underlining different possible loading conditions. Section III presents the experimental setup and the collected data comparing them with model results. Finally, in Section IV the advantages and limits of the presented method are discussed and conclusions are drawn in Section V.

II. Extended SEB model

Following the work of [28], the quasi-static behaviour of a Spine Equivalent Beam in the sagittal plane can be summarized in a set of seven normalized Ordinary Differential Equations (ODEs). Three ODEs are the quasi-static balancing equations in the deformed coordinate system (denoted by $_{123}$) reported in Figure 2 and four equations define the non-linear beam kinematics, two for the displacements (u, w) and two for the rotations (T_{11}, T_{13}). The unknowns are functions of the curvilinear coordinate s. The system could be reduced to a six equations system since the two rotations are dependent. However, an additional equation is beneficial for the numerical solver and has a negligible computational cost.

Describing the stress-free configuration of the spine with a 2D curve with coordinates $(X_0(s), Z_0(s))$ [31], the orientation of the deformed coordinate system can be obtained starting from a fixed one with three rotations: $\boldsymbol{R_{\alpha_0}}$ takes into account hip flexion (α_0), $\boldsymbol{R_0}$ is a consequence of the curved stress-free configuration and $\boldsymbol{R_T}$ results from domain deformation. Therefore, the full rotation matrix $\boldsymbol{R}(\alpha_0, s)$ is

defined as follow:

$$\boldsymbol{R}(\alpha_0, s) = \boldsymbol{R_{\alpha_0}}(\alpha_0) \quad \boldsymbol{R_0}(s) \quad \boldsymbol{R_T}(s) = \\ = \begin{bmatrix} \cos(\alpha_0) & -\sin(\alpha_0) \\ \sin(\alpha_0) & \cos(\alpha_0) \end{bmatrix} \cdot \begin{bmatrix} X_0'(s) & Z_0'(s) \\ -Z_0'(s) & X_0'(s) \end{bmatrix} \\ \cdot \begin{bmatrix} T_{11}(s) & T_{13}(s) \\ -T_{13}(s) & T_{11}(s) \end{bmatrix}, \tag{1}$$

where $(.)'$ stands for $\frac{\mathrm{d}}{\mathrm{d}s}$.

The distributed loads (q_1, q_2, q_3) defined in the deformed coordinate system and applied along the spine are the torso weight ($\boldsymbol{F_t}$) and the Erector-Spine (ES) muscles action. The latter is modelled as a compressive load ($\boldsymbol{F_{ES}}$) function of α_0 (Figure 3), and a distributed moment (m_{ES}). Assuming the arms perpendicular to the ground during the whole flexion cycle, the arms weight corresponds to an external force ($\boldsymbol{F_a}$) at the spine endpoint, whereas the head weight ($\boldsymbol{F_h}$) results in a concentrated force and a concentrated moment. To speed up the numerical convergence, the concentrated loads are distributed along a very short fraction of the spine length (δ). Therefore q_1, q_2, q_3 are defined as follows:

$$\begin{bmatrix} q_1 \\ q_3 \\ q_2 \end{bmatrix} = \begin{bmatrix} \boldsymbol{f} + \boldsymbol{R}(s, \alpha_0)\boldsymbol{F_t} + \boldsymbol{F_{ES}}(\alpha_0) \\ |\boldsymbol{m}| + m_{ES} - |\boldsymbol{R}(s, \alpha_0)\boldsymbol{r_d}(s) \times \boldsymbol{F_{ES}}(\alpha_0)| \end{bmatrix}, \tag{2}$$

where

$$\boldsymbol{f} = \begin{cases} \delta^{-1}\boldsymbol{R}(1, \alpha_0)(\boldsymbol{F_h} + \boldsymbol{F_a}), & s \in [1-\delta, 1] \\ 0, & s \in [0, 1-\delta] \end{cases}, \tag{3}$$

$$\boldsymbol{m} = \begin{cases} \delta^{-1}\boldsymbol{R_0}(1)(\boldsymbol{d_h} \times \boldsymbol{R}(1, \alpha_0)\boldsymbol{F_h}), & s \in [1-\delta, 1] \\ 0, & s \in [0, 1-\delta] \end{cases}, \tag{4}$$

$$\boldsymbol{r_d}(s) = \boldsymbol{R}^T_{\boldsymbol{\alpha_0}}(s)[X_0(s), Z_0(s)]^T + \boldsymbol{R_0}(s)^T[u(s), w(s)]^T, \tag{5}$$

and $\boldsymbol{d_h}$ is the distance vector between the spine endpoint ($s = 1$) and the head centre of mass.

All the quantities are normalized, distances and forces refer to the following normalization equations where $\tilde{(.)}$ stands for dimensional quantities:

$$v = \frac{\tilde{v}}{L}, \quad F = \frac{L^2}{EI_m}\tilde{F}, \tag{6}$$

with L being the undeformed spine length, I_m the maximum value of the area moment of inertia and E the equivalent Young's Modulus. Solving a simplified system at standing ($M_2 = 0$), the distributed moment (m_{ES}) can be written as a function of E. Therefore, matching model prediction and experimental data for an unloaded flexion cycle, m_{ES} and E can be quantified for each subject [28].

While carrying on physical activities, the ES muscles activation provide an extra moment (q_{ES}) needed to retain a certain spine configuration despite additional external loads. Assuming a constant contribution along curvilinear coordinate (s) and measuring the spine rotation at its end point

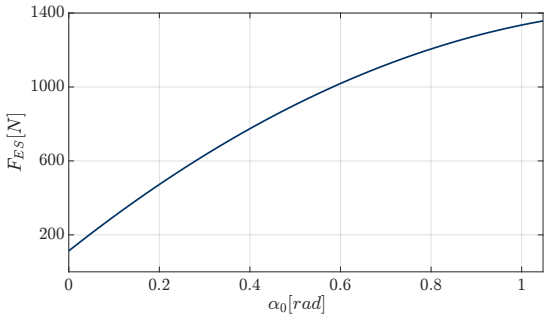

Fig. 3: The Erector-Spine (ES) compressive force (F_{ES}) as a function of the hip rotation (α_0).

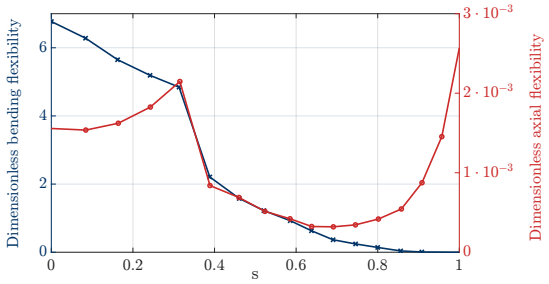

Fig. 4: The dimensionless spine axial flexibility (B) and the dimensionless spine bending flexibility (C) as a function of a curvilinear coordinate (s).

($\overline{T}_{11}$), the extra moment can be quantified solving a system of eight ODEs. The normalized ODEs are:

$$\frac{\mathrm{d}}{\mathrm{d}s}\begin{bmatrix} F_1 \\ F_3 \\ M_2 \\ T_{11} \\ T_{13} \\ u \\ w \\ q_{ES} \end{bmatrix} = \begin{bmatrix} -\rho F_3 - q_1 \\ \rho F_1 - q_3 \\ (1+e)F_3 - q_2 + q_{ES} \\ (\rho - \bar{\rho})T_{13} \\ (\bar{\rho} - \rho)T_{11} \\ -1 - \bar{\rho}w + (1+e)T_{11} \\ \bar{\rho}u + (1+e)T_{13} \\ 0 \end{bmatrix}. \tag{7}$$

The relative curvature $(\rho - \bar{\rho})$ and the axial strain e are defined as:

$$\begin{bmatrix} e \\ \rho - \bar{\rho} \end{bmatrix} = \begin{bmatrix} B & 0 \\ 0 & C \end{bmatrix} \begin{bmatrix} F_1 \\ M_2 \end{bmatrix}, \tag{8}$$

where B is the dimensionless spine axial flexibility and C the dimensionless spine bending flexibility (Figure 4). The latter takes into account the limited range of motion of the upper part of the spine due to the presence of the ribcage [32]. The Boundary Conditions (BCs) are:

$$T_{11} = 1, \quad T_{13} = 0, \quad u = w = 0 \quad for \quad s = 0, \\ F_1 = F_3 = M_2 = 0 \quad T_{11} = \overline{T}_{11} \quad for \quad s = 1. \tag{9}$$

The set of ODEs (7) with their relative BCs (9) form a Boundary Value Problem (BVP) which can be solved numerically using a shooting method [33]. The model solution consists of displacements, rotations and loads defined along the dimensionless domains $s \in [0 \quad 1]$.

The minimum data required for this model are subject's weight (W) and height (h). Biometrics data are scaled using these two values [34]:

$$\begin{bmatrix} |\boldsymbol{F_h}| \\ |\boldsymbol{F_a}| \\ |\boldsymbol{F_t}| \end{bmatrix} = \begin{bmatrix} 0.073 \\ 0.098 \\ 0.507 \end{bmatrix} W, \quad |\boldsymbol{d_h}| = 0.0689{\cdot}h, \quad L = 0.2709{\cdot}h. \tag{10}$$

To quantify the risk associated with lifting and carrying objects while retain a certain posture, additional loads $\boldsymbol{f_e}$, $\boldsymbol{m_e}$ and $\boldsymbol{m_a}$ must be added to the terms $\boldsymbol{f}$ and $\boldsymbol{m}$. Assuming the arms perpendicular to the ground, a weight in hands would result in an additional concentrated force:

$$\begin{aligned} \boldsymbol{f_e} &= \delta^{-1}\boldsymbol{R}(1,\alpha_0)\boldsymbol{F_e} \\ \boldsymbol{m_e} &= \boldsymbol{m_a} = 0 \end{aligned} \tag{11}$$

with $\boldsymbol{F_e} = [-F_e \quad 0]^T$. If the arms are rotated of an angle (β) with respect to the perpendicular to the ground, the same weight leads to an additional concentrated force and additional concentrated moment:

$$\begin{aligned} \boldsymbol{f_e} &= \delta^{-1}\boldsymbol{R}(1,\alpha_0)\boldsymbol{F_e} \\ \boldsymbol{m_e} &= \delta^{-1}(\boldsymbol{R}(1,\alpha_0)\boldsymbol{d_F}(\beta)) \times \boldsymbol{F_e} \\ \boldsymbol{m_a} &= \delta^{-1}(\boldsymbol{R}(1,\alpha_0)\boldsymbol{d_a}(\beta)) \times \boldsymbol{F_a} \end{aligned} \tag{12}$$

with $d_a = [X_0(1) \quad Z_0(1)]^T + \boldsymbol{R}(\beta)[0 \quad l_{arm}/2]^T$ and $d_W = [X_0(1) \quad Z_0(1)]^T + \boldsymbol{R}(\beta)[0 \quad l_{arm}]^T$.
Finally, if the applied load is not parallel to the gravity:

$$\begin{aligned} \boldsymbol{f_e} &= \delta^{-1}\boldsymbol{R}(1,\alpha_0)\boldsymbol{F_e} \\ \boldsymbol{m_e} &= \delta^{-1}(\boldsymbol{R}(1,\alpha_0)\boldsymbol{d_F}(\beta)) \times \boldsymbol{F_e} \\ \boldsymbol{m_a} &= \delta^{-1}(\boldsymbol{R}(1,\alpha_0)\boldsymbol{d_a}(\beta)) \times \boldsymbol{F_a} \end{aligned} \tag{13}$$

with $\boldsymbol{F_e} = [F_e^X \quad F_e^Z]^T$.

III. Experimental analysis

A. Experimental setup

To validate the predicted muscles activity an experimental analysis was conducted. Six healthy volunteers, four males and two females, (age: 27.6 ± 2 years; mass: 65.6 ± 14.3 kg; height: 177.6 ± 6.7 cm)[1] were recruited in the experimental session. Participants were students and researchers with no or limited experience of industrial work. Written informed consent was obtained after explaining the experimental procedure and a numerical ID was assigned to anonymise the data. The whole experimental procedure was carried out at Human-Robot Interfaces and Physical Interaction (HRII) Lab, Italian Institute of Technology (IIT) in accordance with the Declaration of Helsinki, and the protocol was approved by the ethics committee Azienda Sanitaria Locale (ASL) Genovese N.3 (Protocol IIT_HRII_ERGOLEAN 156/2020).

In Figure 5, all the sensor systems employed in the experimental analysis are highlighted. An Xsens MVN Biomech suit was used to measure the whole-body motion. It is a commercial product realised by Xsens Technologies B.V. (Enschede, Netherlands) and equipped with seventeen inter-connected inertial measurement unit (IMU) sensors. The whole-body Centre of Pressure (CoP) and Ground Reaction Force (GRF) were collected using a Kistler force plate, commercialised by Kistler Holding AG (Winterthur, Switzerland). Muscle activity was measured in six locations (L5, L3, L1, T10, T8, T2) along the subject back for the entire duration of the experiment. EMG signals were collected using a Delsys Trigno Wireless system, commercialised by Delsys Inc. (Natick, MA, United States). Afterwards, they were filtered and normalized to maximum voluntary contractions (MVC).

[1]Subject data is reported as: mean ± standard deviation.

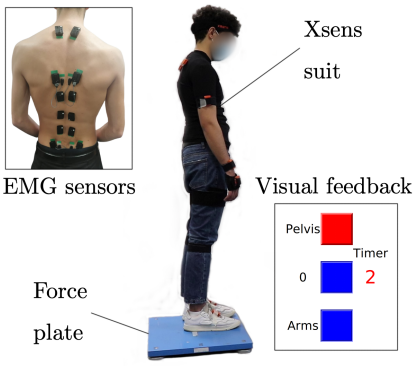

Fig. 5: The experimental set up with all the sensor systems employed and the visual feedback interface provided to the subjects.

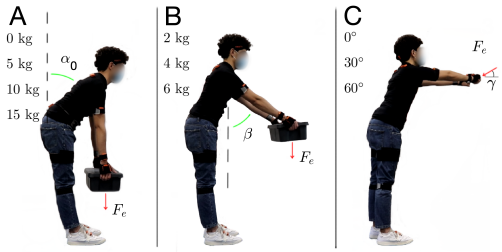

Fig. 6: The three tests performed involving a spine flexion cycle: (A) with the arms perpendicular to the ground, (B) while rotating the arms of an angle β, (C) with a load not parallel to gravity.

Three tests were carried out to address different loading conditions. In Figure 6, the three experimental setups are illustrated. In the first test, the subjects were asked to perform a full flexion cycle with the spine maintaining the arms perpendicular to the ground. The desired α_0 was indicated to the subjects during the test through a visual feedback interface (see Figure 5). Whether the measured angle was too high or too low, the coloured square was red or blue, respectively, while it turned into green when it matched the admissible range ($\pm 1.5°$). $\overline{T}_{11}$, instead, depended on the subjects' range of motion and was measured but not prescribed. The test was repeated

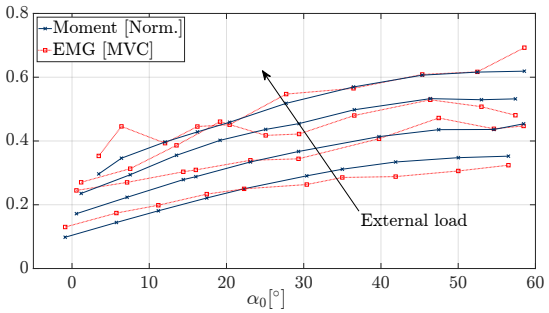

Fig. 7: Predicted and measured muscles activities as a function of the hip rotation, α_0, during test A in four different loading conditions (0 kg, 5 kg, 10 kg, 15 kg) for subject 1.

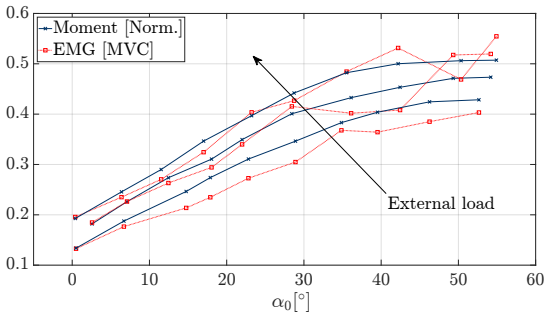

Fig. 8: Predicted and measured muscles activities as a function of the hip rotation, α_0, during test B in three different loading conditions (2 kg, 4 kg, 6 kg) for subject 1.

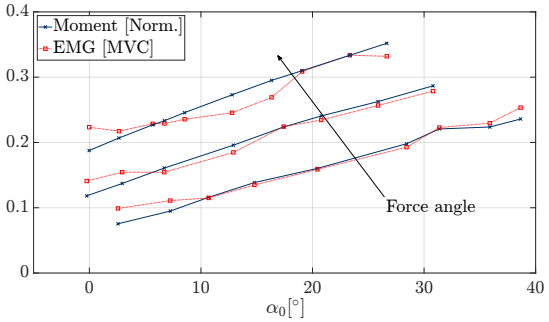

Fig. 9: Predicted and measured muscles activities as a function of the hip rotation, α_0, during test C in three different load orientations (0°, 30°, 60°) for subject 1.

four times with different weights in hands (0 kg, 5 kg, 10 kg, 15 kg). In the second test, to transfer the moment, the spine flexion cycle was then performed while rotating the arms of an angle β. Both the desired α_0 and the desired β were indicated to the subjects during the test through the visual feedback interface. The test was repeated three times considering loads of 2 kg, 4 kg, 6 kg, respectively. Finally, a load not parallel to gravity was experienced by the subjects in the third test. The external force was measured with a Mini45 F/T sensor, commercialized by ATI Industrial Automation (headquarters: Apex, NC, United States). The subjects were provided with a visual feedback interface to convey, this time, the magnitude of the experienced force. A constant force, $\simeq$ 40N, was prescribed for all the tests while the force orientation changed. The load orientation was selected with an angle γ equal to 0°, 30° and 60°, respectively.

B. Results

The numerically predicted normalized moments required to retain a specific configuration (q_{ES}) were compared with the scaled EMG signals. The values reported in Figure 7, 8, 9 represent the average values among all locations for one subject (Subject 1). Figure 7 shows predicted and measured muscles activities during the first test in four different loading conditions. As the hip flexion increased (α_0), the distributed moment required to match the rotation $\overline{T}_{11}$ increased as well. Besides, curves related to higher external loads are shifted towards higher activities. It is worth noticing that each point corresponds to a couple of $(\alpha_0, \quad \overline{T}_{11})$ while the 2D plot reports only the most relevant variable, namely (α_0).

Figure 8 refers to test B where three different loading conditions were considered. The arms rotation led to a higher external moment during the flexion cycle. As a consequence, the test resulted more demanding and the curves rose faster than the previous loading condition. In the third test, the external force magnitude was constant ($\simeq$ 40N) and the force orientation changed (Figure 9). The three orientations tested were horizontal (lower activity), 30° and 60° with respect to the horizontal (higher activity).

For each couple of curves, the relative error in the predicted muscle activity can be computed as follow:

$$e = \frac{1}{N}\sum_{1}^{N}\frac{|y_{EMG} - q_{ES}|}{y_{EMG}} \tag{14}$$

where y_{EMG} is the measured muscle activity and N the number of points in the curve. Each test was repeated twice, leading to eight couples of curves relative to test A and six to test B and test C. Figure 10 summarizes the relative error for each subject and the value averaged among all the subjects in the three tests. The muscle activity can be predicted with an average accuracy around the 10% of the measured values, similarly for the three different tests. A maximum relative error greater than 20% was reported for Subject 6 while the first two subjects showed relative errors similar to the 5% of the measured values. A statistical analysis was performed to verify the significance of these results, considering a level of statistical significance equal to 0.05. The one-way analysis of variance (ANOVA) was applied to the EMG signals while the non-parametric Kruskal-Wallis test was applied to the predicted moment due to a lack of normality in the data. The aim was to examine the differences among the experimental conditions (i.e., external load magnitude or direction). Since significant results were found between the conditions for all the tests, post-hoc pairwise comparisons were also made with Bonferroni correction for multiple comparisons. Figure 11

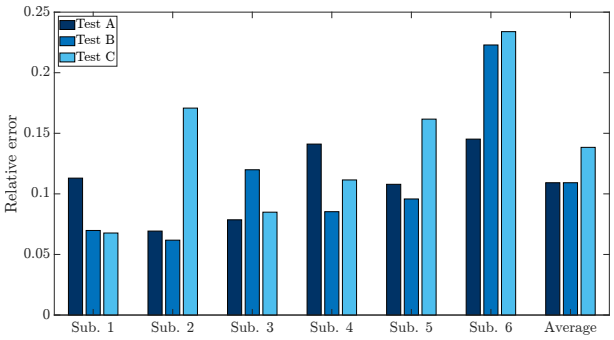

Fig. 10: Relative error for each subject in three performed tests and average values across all the subjects.

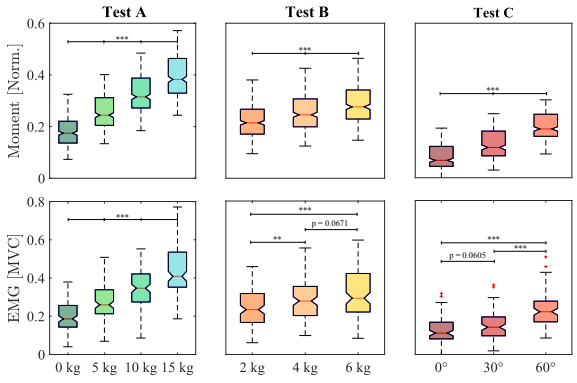

Fig. 11: Box plots of the predicted (first line) and measured (second line) muscles activities averaged among all the subjects for the three test performed (A, B and C). For each test, the box plots represent the different experimental conditions. Asterisks indicate the level of statistical significance after post-hoc tests: $^{*}p < 0.05$, $^{**}p < 0.01$ and $^{***}p < 0.001$

illustrates the box plots of the predicted and measured muscle activity averaged among all the subjects. The pairwise differences between experimental conditions, examined by the statistical tests, are reported in Figure 11 thorough dedicated bars on the top of the box plots.

IV. Discussion

During physical activities, the rise of the compressive forces acting along the spine is due to two different contributes: direct load reaction and muscle contraction. In this work, we propose a computationally inexpensive tool able to locally quantify the direct effect of an external load and to estimate the muscle activation related to a certain body configuration. Thus, the risk associated with both these aspects is taken into account.

As clearly represented in Figure 11, the trend of the computed normalized moment to vary external forces was comparable to the trend of the EMG measurements in all the tests performed. Thus the proposed model proved its capability to predict human muscle activity and account for different loading conditions. Furthermore,

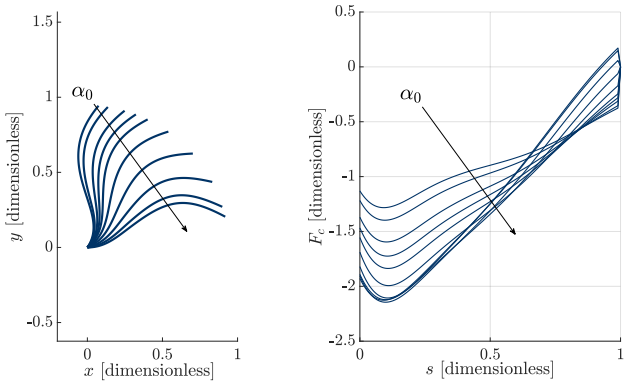

Fig. 12: On the left: the spine configuration during test B (6 kg in hands). On the right: the relative compressive force distribution.

statistically significant differences were found among all the experimental conditions for the predicted muscle activity and among most of the conditions for the measured one. The only exceptions were for the EMG signals in Test B (4 kg versus 6 kg) and Test C (0° versus 30°). Although the most relevant requirements were prescribed during the three experimental tests, replicating the same body configurations for all the experimental conditions resulted extremely challenging. The subject's effort during the tests highly depended on the body configuration. Therefore, the significance of the EMG values grouped by the only external weight could be undermined.

Limiting the analysis to the simplest loading condition, the quantified compressive forces were validated against in-vivo measurements in [28]. Figure 12 reports the spine configuration and the compressive force distribution for different values of α_0 during the second experiment (6 kg in hands). If compared with the case with no weight in hands and no arms rotation, the graph on the right shows a maximum loading larger than the 40%. This condition might be critical for the subjects. Nevertheless, it is not possible to define a general threshold since critical values are highly subject-dependent. Therefore, a similar online assessment method could feedback the risks level associated with compressive load and muscle activity, but subject-specific limits must also be defined.

While the direct effect of an external load can be quantified under the model assumptions, the compressive loading resulting from muscles activation must be scaled with the activation level. Furthermore, the presented approach is limited to motions taking place in the sagittal plane and loading condition symmetric to this plane. In the experimental setup, we took advantage of a full suit for reconstructing the links orientations. However, the number of sensors can be reduced up to four: two for capturing the rotation at the beginning and the end of the worker back, and two to define the arms configuration. Finally, the numerical solution of the BVP requires few seconds, so it

is suitable for the online assessment of activities with low dynamics.

Our main focus is a practical tool suitable to monitor spine compressive loading of a large number of workers during physical tasks. It is meant to be employed outside the lab providing online risk assessment capabilities in real working environments. To quantify the effect of an external load on a flexible body, 3D geometries finely discretized could result in more accurate subject-specific stresses. However, defining and calibrating similar numerical models for a large number of subjects would result in an unacceptable set-up time. In addition, solutions must be obtained in a short amount of time to perform online assessments, so model accuracy is highly dependent on the available computational power.

V. Conclusion

In the manufacturing sector, LBP is a frequent chronic condition among workers. During physical activities, the back supports a recurring compressive load. Being the main risk factor, monitoring the compressive forces along the spine could largely reduce the number of workers affected by this MSD. Therefore, we proposed an online method to quantify the risk associated with a measured posture and a known handled weight. The extended SEB model can quantify the spine compressive forces as a function of space, and estimate the required muscle activity. The estimated ES muscles action has been validated against experimental data showing an average relative accuracy of 10%.

The presented approach requires a minimum set of four inertia sensors, relative small computational resources and a very limited amount of input data. These advantages make it suitable for a real working scenario and a large number of subjects. Furthermore, it can be further specialized on-demand adding subject-specific data, like the spine initial curvature or subject-specific body segments lengths, and different strategies can be prescribed to the subjects.

In industry 4.0, smart factories can take advantage of autonomous systems to promote ergonomic tasks and safeguard employees' health. The frequency of human-robot physical interactions will keep on increasing with the number of available robotics solutions. In the next decades, fostering human-centred collaborative robotics is one primary target since both social and economical conditions would be improved. An online method can promote preventive strategies, and cobots can plan tasks execution minimizing the risk associated with high spine compressive loading. Alternatively, exoskeletons expanding humans capabilities can also fight work-related MSDs, and control strategies of active exoskeletons can rely on online model solutions.

VI. Acknowledgements

This work was supported in part by the European Research Council (ERC) starting grant Ergo-Lean, (GA 850932), and by the European Union's Horizon 2020 research and innovation programme SOPHIA (GA 871237).

References

[1] S. Niu, "Ergonomics and occupational safety and health: An ILO perspective," *Applied Ergonomics*, vol. 41, no. 6, pp. 744–753, 2010. [Online]. Available: http://dx.doi.org/10.1016/j.apergo.2010.03.004

[2] M. Bair, R. Robinson, W. Katon, and K. Kroenke, "Depression and pain comorbidity - A literature review," *ARCHIVES OF INTERNAL MEDICINE*, vol. 163, no. 20, pp. 2433–2445, NOV 10 2003.

[3] S. Bevan, "Economic impact of musculoskeletal disorders (MSDs) on work in Europe," *Best Practice and Research: Clinical Rheumatology*, vol. 29, no. 3, pp. 356–373, 2015. [Online]. Available: http://dx.doi.org/10.1016/j.berh.2015.08.002

[4] W. F. Stewart, J. A. Ricci, E. Chee, D. Morganstein, and R. Lipton, "Lost Productive Time and Cost Due to Common Pain Conditions in the US Workforce," *Journal of the American Medical Association*, vol. 290, no. 18, pp. 2443–2454, 2003.

[5] W. S. Marras, "Occupational low back disorder causation and control," *Ergonomics*, vol. 43, no. 7, pp. 880–902, 2000.

[6] L. Gualtieri, E. Rauch, and R. Vidoni, "Emerging research fields in safety and ergonomics in industrial collaborative robotics: A systematic literature review," *Robotics and Computer-Integrated Manufacturing*, vol. 67, p. 101998, 2021.

[7] E. Matheson, R. Minto, E. G. Zampieri, M. Faccio, and G. Rosati, "Human-robot collaboration in manufacturing applications: A review," *Robotics*, vol. 8, no. 4, pp. 1–25, 2019.

[8] S. Kana, K.-P. Tee, and D. Campolo, "Human-Robot co-manipulation during surface tooling: A general framework based on impedance control, haptic rendering and discrete geometry," *ROBOTICS AND COMPUTER-INTEGRATED MANUFACTURING*, vol. 67, FEB 2021.

[9] L. Peternel, C. Fang, N. Tsagarakis, and A. Ajoudani, "A selective muscle fatigue management approach to ergonomic human-robot co-manipulation," *Robotics and Computer-Integrated Manufacturing*, vol. 58, no. June 2018, pp. 69–79, 2019. [Online]. Available: https://doi.org/10.1016/j.rcim.2019.01.013

[10] D. J. Agravante, A. Cherubini, A. Bussy, P. Gergondet, and A. Kheddar, "Collaborative human-humanoid carrying using vision and haptic sensing," *Proceedings - IEEE International Conference on Robotics and Automation*, no. October 2015, pp. 607–612, 2014.

[11] X. Yu, W. He, Q. Li, Y. Li, and B. Li, "Human-robot co-carrying using visual and force sensing," *IEEE Transactions on Industrial Electronics*, pp. 1–1, 2020.

[12] W. Kim, J. Lee, N. Tsagarakis, and A. Ajoudani, "A real-time and reduced-complexity approach to the detection and monitoring of static joint overloading in humans," in *Rehabilitation Robotics (ICORR), 2017 International Conference on*. IEEE, 2017, pp. 828–834.

[13] L. Fortini, M. Lorenzini, W. Kim, E. De Momi, and A. Ajoudani, "A real-time tool for human ergonomics assessment based on joint compressive forces," in *2020 International Conference on Robot & Human Interactive Communication (RO-MAN)*. IEEE, 2020.

[14] M. Lorenzini, W. Kim, E. D. Momi, and A. Ajoudani, "A new overloading fatigue model for ergonomic risk assessment with application to human-robot collaboration," *Proceedings - IEEE International Conference on Robotics and Automation*, vol. 2019-May, pp. 1962–1968, 2019.

[15] L. Peternel, N. Tsagarakis, D. Caldwell, and A. Ajoudani, "Robot adaptation to human physical fatigue in human-robot co-manipulation," *AUTONOMOUS ROBOTS*, vol. 42, no. 5, SI, pp. 1011–1021, JUN 2018.

[16] W. Kim, L. Peternel, M. Lorenzini, J. Babič, and A. Ajoudani, "A human-robot collaboration framework for improving ergonomics during dexterous operation of power tools," *Robotics and Computer-Integrated Manufacturing*, vol. 68, p. 102084, 2021.

[17] W. Kim, M. Lorenzini, P. Balatti, P. D. Nguyen, U. Pattacini, V. Tikhanoff, L. Peternel, C. Fantacci, L. Natale, G. Metta, and A. Ajoudani, "Adaptable Workstations for Human-Robot Collaboration: A Reconfigurable Framework for Improving Worker Ergonomics and Productivity," *IEEE Robotics and Automation Magazine*, vol. 26, no. 3, pp. 14–26, 2019.

[18] J. H. Van Dieën, H. Weinans, and H. M. Toussaint, "Fractures of the lumbar vertebral endplate in the etiology of low back pain: A hypothesis on the causative role of spinal compression in aspecific low back pain," *Medical Hypotheses*, vol. 53, no. 3, pp. 246–252, 1999.

[19] A. Rohlmann, M. Dreischarf, T. Zander, F. Graichen, P. Strube, H. Schmidt, and G. Bergmann, "Monitoring the load on a telemeterised vertebral body replacement for a period of up to 65 months," *EUROPEAN SPINE JOURNAL*, vol. 22, no. 11, pp. 2575–2581, NOV 2013.

[20] J. M. Warren, A. P. Mazzoleni, and L. A. Hey, "Development and validation of a computationally efficient finite element model of the human lumbar spine: Application to disc degeneration," *International Journal of Spine Surgery*, vol. 14, no. 4, pp. 502–510, 2020. [Online]. Available: http://www.ijssurgery.com/content/14/4/502

[21] E. Wagnac, P.-J. Arnoux, A. Garo, and C.-E. Aubin, "Finite element analysis of the influence of loading rate on a model of the full lumbar spine under dynamic loading conditions," *MEDICAL & BIOLOGICAL ENGINEERING & COMPUTING*, vol. 50, no. 9, pp. 903–915, SEP 2012.

[22] A. Rohlmann, L. Bauer, T. Zander, G. Bergmann, and H. J. Wilke, "Determination of trunk muscle forces for flexion and extension by using a validated finite element model of the lumbar spine and measured in vivo data," *Journal of Biomechanics*, vol. 39, no. 6, pp. 981–989, 2006.

[23] F. Ghezelbash, A. Shirazi-Adl, Z. El Ouaaid, A. Plamondon, and N. Arjmand, "Subject-specific regression equations to estimate lower spinal loads during symmetric and asymmetric static lifting," *JOURNAL OF BIOMECHANICS*, vol. 102, no. SI, MAR 26 2020, 3rd International Workshop on Spinal Loading and Deformation, Charite Univ Berlin, Julius Wolff Inst, Berlin, GERMANY, JUL 04-06, 2019.

[24] S. S. W. Li, C. C. F. Chu, and D. H. K. Chow, "EMG-based lumbosacral joint compression force prediction using a support vector machine," *MEDICAL ENGINEERING & PHYSICS*, vol. 74, pp. 115–120, DEC 2019.

[25] K. P. Granata and W. S. Marras, "An EMG-assisted model of trunk loading during free-dynamic lifting," *Journal of Biomechanics*, vol. 28, no. 11, pp. 1309–1317, 1995.

[26] N. Arjmand, D. Gagnon, A. Plamondon, A. Shirazi-Adl, and C. Larivière, "Comparison of trunk muscle forces and spinal loads estimated by two biomechanical models," *Clinical Biomechanics*, vol. 24, no. 7, pp. 533–541, 2009. [Online]. Available: http://dx.doi.org/10.1016/j.clinbiomech.2009.05.008

[27] A. Garo, P. J. Arnoux, E. Wagnac, and C. E. Aubin, "Calibration of the mechanical properties in a finite element model of a lumbar vertebra under dynamic compression up to failure," *MEDICAL & BIOLOGICAL ENGINEERING & COMPUTING*, vol. 49, no. 12, pp. 1371–1379, DEC 2011.

[28] Y. Xie and K. M. Lee, "Spine-Equivalent Beam Modeling Method with in Vivo Validation for the Analysis of Sagittal Standing Flexion," *IEEE/ASME Transactions on Mechatronics*, vol. 25, no. 4, pp. 2075–2087, 2020.

[29] J. H. Van Dieën, I. Kingma, and J. C. Van Der Bug, "Evidence for a role of antagonistic cocontraction in controlling trunk stiffness during lifting," *Journal of Biomechanics*, vol. 36, no. 12, pp. 1829–1836, 2003.

[30] J. Cholewicki, S. M. McGill, and R. W. Norman, "Comparison of muscle forces and joint load from an optimization and EMG assisted lumbar spine model: Towards development of a hybrid approach," *Journal of Biomechanics*, vol. 28, no. 3, 1995.

[31] A. Bruno, M. Bouxsein, and D. Anderson, "Development and validation of a musculoskeletal model of the fully articulated thoracolumbar spine and rib cage," *Journal of biomechanical engineering*, vol. 137, 04 2015.

[32] C. Liebsch, N. Graf, K. Appelt, and H.-J. Wilke, "The rib cage stabilizes the human thoracic spine: An in vitro study using stepwise reduction of rib cage structures," *PLOS ONE*, vol. 12, no. 6, pp. 1–13, 06 2017. [Online]. Available: https://doi.org/10.1371/journal.pone.0178733

[33] W. H. Press, S. A. Teukolsky, W. T. Vetterling, and B. P. Flannery, *Numerical Recipes 3rd Edition: The Art of Scientific Computing*, 3rd ed. USA: Cambridge University Press, 2007.

[34] C. E. Clauser, J. T. McConville, and J. W. Young, "Weight, volume, and center of mass of segments of the human body," Antioch Coll Yellow Springs OH, Tech. Rep., 1969.